Hindawi
Advances in Civil Engineering
Volume 2019, Article ID 3965803, 13 pages
https://doi.org/10.1155/2019/3965803

Research Article

A Fractal Model to Interpret Porosity-Dependent Hydraulic Properties for Unsaturated Soils

Annan Zhou,[1] **Yang Fan**,[2] **Wen-Chieh Cheng**,[3] **and Junran Zhang**[4]

[1]*School of Engineering, Royal Melbourne Institute of Technology (RMIT), Melbourne, VIC 3001, Australia*
[2]*School of Transportation Science and Engineering, Beihang University, Beijing 100191, China*
[3]*School of Civil Engineering, Xi'an University of Architecture and Technology, Xi'an 710055, China*
[4]*Henan Province Key Laboratory of Geomechanics and Structural Engineering, North China University of Water Resources and Electric Power, Zhengzhou, Henan 450045, China*

Correspondence should be addressed to Annan Zhou; annan.zhou@rmit.edu.au

Received 14 June 2018; Accepted 12 November 2018; Published 8 January 2019

Academic Editor: Castorina S. Vieira

This paper presents a simple fractal model to quantify the effects of initial porosity on the soil-water retention curve and hydraulic conductivity of unsaturated soils. In the proposed conceptual model, the change of maximum pore radius, which largely determines the change of the air-entry value, is directly related to the fractal dimension of pore volume (D) and porosity change. The hydraulic properties of unsaturated soils are then governed by the maximum pore radius, the fractal dimension of pore volume (D), and the fractal dimension of drainable pore volume ($D_d \leq D$). The new fractal model removes the empirical fitting parameters that have no physical meaning from existing models for porosity-dependent water retention and hydraulic behaviour and employs parameters of fractal dimensions that are intrinsic to the nature of the fractal porous materials. The proposed model is then validated against experimental data from the literature on soil-water retention behaviour and unsaturated conductivity.

1. Introduction

Hydraulic properties usually refer to the properties that are related to the water retention behaviour and the hydraulic conductivity of soil, which have numerous applications in geotechnical engineering [1–6]. Soil-water retention behaviour is usually described by the soil-water retention curve (SWRC or the soil-water characteristic curve, SWCC), which is defined as the relationship between the effective degree of saturation, S_e, and the matric suction, s. Conversely, the hydraulic conductivity of soil is commonly described using the hydraulic conductivity function (HCF), which is defined as the relationship between the relative coefficient of conductivity, K_r (the ratio between the unsaturated and saturated values, K/K_s), and the matric suction, s, or the effective degree of saturation, S_e. It is generally recognised that the hydraulic conductivity for unsaturated soils can be effectively estimated using the soil-water retention curve, which is one of the most important applications of SWRC [7].

Numerous equations have been proposed to model SWRCs for partially saturated soils [7–11] and for HCFs [7, 11–14]. Some of these equations are based on a functional regression of the experimental data, while others are based on empirical correlations with other soil properties, such as particle or pore-size distribution, porosity, and specific surface area. However, concerns are often raised about the empirical nature of those models because they do not shed any light on the fundamental physical principles that govern the processes of unsaturated flow and drainage [15]. Several physical models for soil hydraulic properties based on the concept of fractal geometry for soil texture and pore structure have been developed [15–24]. The most important motivation to develop fractal SWRC models and fractal HCF models is that these models are able to remove the empirical fitting parameters that have no physical meaning and employ parameters of fractal dimensions that are intrinsic to the nature of the fractal porous materials [15].

One specific factor that affects the SWRC and HCF is the porosity (ϕ) or void ratio ($e = \phi/(1-\phi)$) of the soil. A change

in soil porosity can lead to a significant change in the SWRC and HCF (experimental evidence can be found in the studies of Croney and Coleman [25] and Laliberte et al. [26]); such a change is a common feature of natural soils [27]. However, it is difficult to justify that samples of a given soil with different porosities should be treated as entirely different soils for modelling. Nevertheless, most of the empirical and fractal SWRC and HCF models mentioned above omit the porosity dependency of soil hydraulic properties.

The issue of the effects of porosity on the hydraulic properties of soil was perhaps first raised by Croney and Coleman [25] and then followed by Laliberte et al. [26]. Recently, the study of the porosity effects on hydraulic properties of unsaturated soils has attracted much attention because of the rapid development of unsaturated soil mechanics involving hydromechanical coupling [28–38]. In the literature, a few approaches have been proposed to model the effect of soil porosity on SWRCs and HCFs. For example, Gallipoli et al. [28] suggested including a function of specific volume (v) in the SWRC equation proposed by Van Genuchten [11]. Assouline suggested an empirical approach based on regression that could model the effects of an increasing soil bulk density on the soil-water retention curve (SWRC) and the hydraulic conductivity function (HCF) [27, 39]. Sun et al. proposed a hydraulic model where a change in the degree of saturation (S_r) can be caused by a change in the matric suction or a change in soil volume (v) [40, 41]. Masin [30] proposed a hydraulic model that can predict the dependency of the degree of saturation (S_r) on the void ratio (e) using the effective stress principle. Tarantino [42] proposed a SWRC equation for deformable soils based on an empirical power function of the water ratio (e_w). Very recently, Sheng and Zhou [43] and Zhou et al. [44] proposed an incremental relationship between the degree of saturation (S_r) and the void ratio (e) by realising that the SWRC is obtained under constant stress instead of constant volume.

However, almost all these approaches are based on phenomenological methodology. Therefore, the modelling parameters used to interpret the dependency of SWRC and HCF on the initial void ratio (e.g., parameters ϕ and ψ in Gallipoli et al. [28]; parameter λ_{se} in Sun et al. [45]; parameter λ_{p0} in Masin [30]; and parameter ζ in Zhou et al. [44]) lack any physical meaning and depend on experimental observations. In this paper, we propose a simple physical model based on fractal geometry to quantify the effects of initial porosity on the soil-water retention curve (SWRC) and the hydraulic conductivity function (HCF) of unsaturated soils. The proposed porosity-dependent SWRC and HCF models only require three parameters: the air-entry value at a specific initial void ratio (s^*_{ae}), the fractal dimension of pore volume (D), and the fractal dimension of drainable pore volume (D_d).

2. Theory and Presentation of the Model

2.1. Fractal Porous Medium. As shown in Figure 1, a porous medium (V_0) contains a broad range of pore sizes, which decrease in the mean radius from r_0 to r_u ($u >> 1$) and in pore volume from P_0 (the volume of the maximum pore) to P_u (the volume of the minimum pore). The pores are further divided into two categories [46, 47]: interparticle pores (including interaggregate macropores and intraaggregate micropores), which can be deformed via external loads and dewatered by the capillary process or heating, and intraparticle pores, which contain water that is strongly bounded with soil solids. Mercury intrusion porosimetry (MIP) test can be employed to determine the distribution of interparticle pores of soil [48]. During the test, mercury was compressed into pores with different radii at different intrusion pressures. The MIP technique has been widely used for geomaterials like soils. The major limitations of MIP technique include (1) it can only measure the largest available access to a pore (i.e., the size of the entrance towards a pore; for most cases, the entrance size to a pore can be substantially smaller than the inner pore size.) and (2) all the calculations are based on the assumption of cylinder pores. Intraparticle pores are nondeformable, and the intraparticle pore water cannot be dehydrated in the context of this research. In other words, strongly bounded water can be approximately considered a part of the soil solids (V_m in Figure 1) in this research. The mean radius of the interparticle pores decreases from r_0 to r_{m-1}, and the pore volume decreases from P_0 to P_{m-1}. The mean radius of the interparticle pores decreases from r_m to r_u, and the pore volume decreases from P_m to P_u.

Following Rieu and Sposito [22], a real porous medium can be assumed to be a fractal medium in which there is self-similarity of the pore radius in the entire domain from r_0 to r_u. In terms of pore space, we assume that

$$\begin{aligned} r_{i+1} &= \gamma r_i, \\ P_{i+1} &= \gamma^E P_i, \end{aligned} \tag{1}$$

where E is the Euclidean dimension, which is equal to 2 for two-dimensional objects (such as the Sierpinski triangle and the Sierpinski carpet) and 3 for three-dimensional objects (such as the Menger sponge), respectively. γ is a linear similarity ratio that is introduced to describe the scaling property of a fractal medium. For example, γ is equal to 1/3 for the Sierpinski carpet (Figure 2) and 1/2 for the Sierpinski triangle, respectively. V_i is defined as the i^{th} self-similar partial volume, which contains all pores that have a radius $\le r_i$. V_{m-1} is the self-similar partial volume that contains the smallest interparticle pores (radius r_{m-1}) and V_m, which stands for the volume of a soil solid particle that is nondeformable and contains all of the intraparticle pores. If the i^{th} self-similar partial volume can be represented by its mean radius R_i, similar to pores in the fractal medium [22], we have

$$\begin{aligned} R_{i+1} &= \gamma R_i, \\ V_{i+1} &= \gamma^E V_i. \end{aligned} \tag{2}$$

The self-similarity property of a fractal porous medium means that the $(i+1)^{th}$ self-similar partial volume repeats the same pore property of the i^{th} self-similar partial volume. For example, for the Sierpinski carpet (Figure 2), V_0 contains 1 P_0 and 8 ($=3^2-1$) V_1, V_1 contains 1 P_1 and 8 V_2, ..., V_{m-1} contains 1 P_{m-1} and 8 V_m. In general, such a self-similarity can be written as

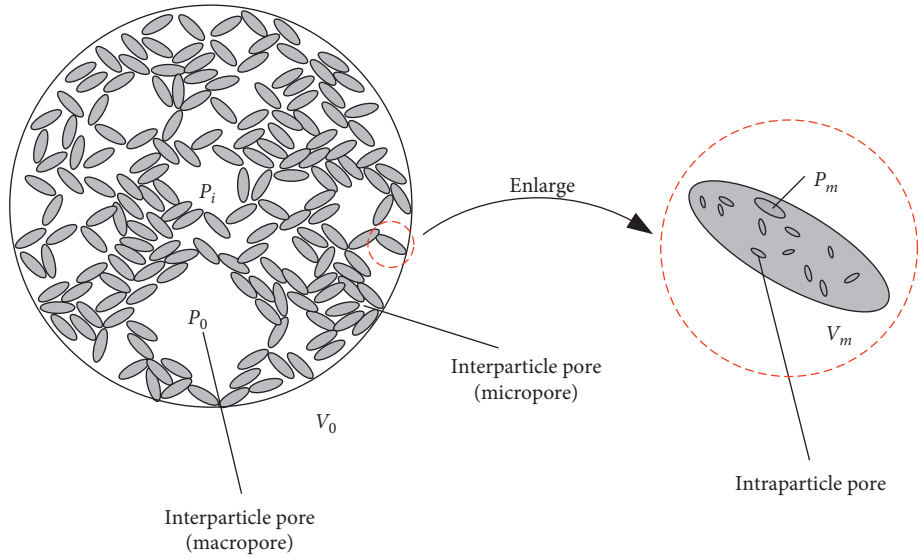

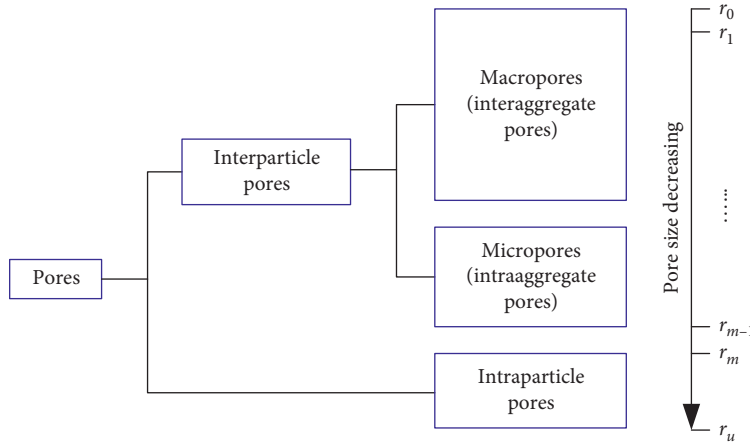

Figure 1: Characterization of pores.

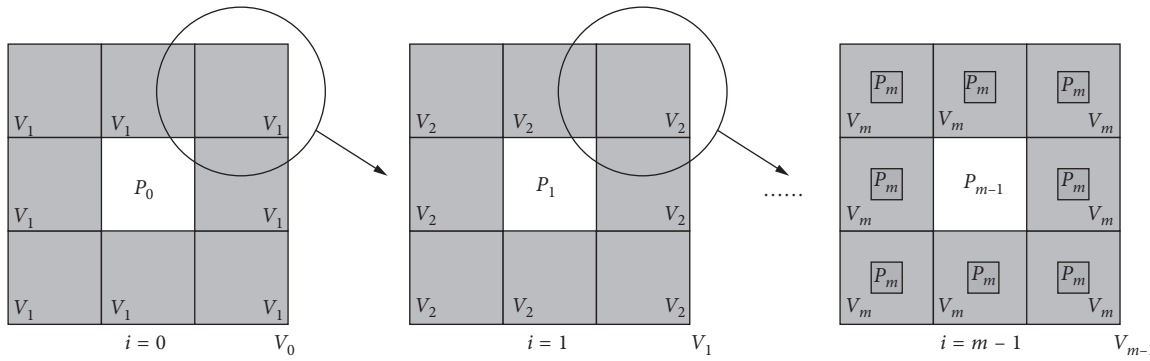

Figure 2: Schematic diagram of fractal porous medium (Sierpinski carpet).

$$V_i = NV_{i+1} + P_i, \tag{3}$$

where a constant number N stands for the number of the $(i + 1)^{\text{th}}$ self-similar partial volume in the i^{th} self-similar partial volume. For the Sierpinski carpet, as shown in Figure 2, $N = 8$. According to equation (3), the total volume V_0 can be written as

$$V_0 = \sum_{i=0}^{m-1} N^i P_i + N^m V_m, \tag{4}$$

where $N^m V_m$ stands for the total solid volume (V_s) in this porous medium. In addition, the pore coefficient Γ is defined as the ratio between the i^{th} pore volume and the i^{th} self-similar partial volume, i.e., $\Gamma = P_i/V_i$. $\Gamma = (1/3)^2$ for the

Sierpinski carpet. V_{i+1}/V_i can be written as a function of Γ, i.e.,

$$\frac{V_{i+1}}{V_i} = \frac{1-\Gamma}{N}. \tag{5}$$

Combining equations (4) and (5) generates

$$\frac{V_m}{V_0} = \frac{V_m}{V_{m-1}}\frac{V_{m-1}}{V_{m-2}}\cdots\frac{V_2}{V_1}\frac{V_1}{V_0} = \frac{(1-\Gamma)^m}{N^m}. \tag{6}$$

According to equation (6), the porosity of the medium thus can be written as

$$\phi = \frac{V_0 - V_s}{V_0} = \frac{V_0 - N^m V_m}{V_0} = 1-(1-\Gamma)^m. \tag{7}$$

For a fractal medium, in terms of pore volume distribution, the number of N and the linear similarity ratio γ can be related through the fractal dimension D [49] of pore space:

$$D_v \equiv \frac{\log N}{\log(1/\gamma)} \text{ or } N = \gamma^{-D}. \tag{8}$$

As mentioned in the study of Gimenez [50], the fractal dimension D of pore volume can be measured using two-dimensional images of cross sections of soils with either the box-counting technique or by the pore size count [51, 52].

Combining equations (2), (5), and (8), we have

$$\frac{V_{i+1}}{V_i} = \frac{1-\Gamma}{N} = \gamma^E \longrightarrow \Gamma = 1-\gamma^{E-D} \text{ or } 1-\Gamma = \gamma^{E-D}. \tag{9}$$

Therefore, the porosity of the medium can be rewritten by substituting equation (9) into equation (7):

$$\phi = 1-\left(\gamma^m\right)^{E-D}. \tag{10}$$

According to equation (1), γ^m can be replaced by r_m/r_0. Therefore, equation (10) can be rewritten as

$$\phi = 1-\left(\frac{r_m}{r_0}\right)^{E-D} \quad (0<D<E), \tag{11}$$

where r_m is the radius of maximum intraparticle pores, which is a constant because the soil particles are assumed as nondeformable. It also augured that equation (11) disagrees with the porosity equation proposed by Katz and Thompson [53] and results in zero porosity when $D=E$ and, therefore, questioned its validity. However, Hunt [54] concluded that Katz and Thompson's model and Rieu and Sposito's model (equation (11)) can be precisely compatible if Katz and Thompson's model involves solid structures and Rieu and Sposito's model involves pore spaces. As mentioned in the study of Hunt [54]; Rieu and Sposito's model is valid for the pore space and Katz and Thompson's cannot be valid if D refers to the pore space. Therefore, it is important to note that the fractal dimension (D) here refers to the pore space other than the solid space in this research. In fact, the condition $D=E$ does not happen for soils in the real world. Experimental evidence [50] shows that the fractal dimensions for various soils are less than the Euclidean dimension. Therefore, Perrier et al. [21] added a boundary condition for equation (11), which always requires $0<D<E$. This boundary condition is also adopted in this article.

According to Xu and Xia [55], the fractal dimension can be assumed to be independent of the soil porosity. Therefore, the porosity change only changes the value of r_0 in equation (11). The change of r_0 will lead to the change of the entire interparticle pore system. The maximum interparticle pore radius is r_0' if the porosity changes from ϕ to ϕ', and r_0' can be written as

$$\frac{r_0'}{r_0} = \left(\frac{1-\phi}{1-\phi'}\right)^{1/(E-D)}. \tag{12}$$

2.2. Porosity-Dependent SWRC. Water in the interparticle pores can be drained by applying soil matric suction. If the fractal porous medium containing interparticle pores with radius $> r_i$ is completely dried due to the capillary flow process, the volumetric water content θ_i can be written as

$$\theta_i = \frac{\sum_{i=i}^{m-1} N^i P_i}{V_0}. \tag{13}$$

However, some interparticle pores with radius $> r_i$ may be isolated by solids and pores with a radius less than r_i. As drying occurs, not all pores of a given size drain at the appropriate suction because of incomplete pore connectivity [56, 57]. The number of drained pores, N_d, is assumed to be fractal and proportional to the power of $(1/\gamma)$, as expressed by

$$N_d = \gamma^{-D_d} \le \gamma^{-D} = N, \tag{14}$$

where D_d ($\le D$) is the fractal dimension for the drainable pore space defined by Perfect [57] and Cihan et al. [56]. Theoretically, D_d is equal to $D - \log(P_d)/\log(\gamma)$, where P_d is the scale-invariant drainage probability for the pore network [57]. Experimentally, D_d can be estimated from the water retention curve; for example, Crawford et al. [58] reported D_d values ranging from 2.90 to 2.97 ($E=3$) along with corresponding D values (obtained from thin section analysis) of between 2.94 and 2.98, for eight Japanese soils.

Therefore, volumetric water content θ_i can be revised as

$$\theta_i = \frac{\sum_{i=0}^{m-1} N^i P_i - \sum_{i=0}^{i-1} N_d^i P_i}{V_0}. \tag{15}$$

Equation (13) is a special case of equation (15) when $N_d = N$. The porosity ϕ, which is related to D rather than D_d, can also be expressed similarly:

$$\phi = \frac{V_0 - V_s}{V_0} = \frac{\sum_{i=0}^{m-1} N^i P_i}{V_0}. \tag{16}$$

Comparing equations (15) and (16) yields

$$\frac{\theta_i}{\phi} = \frac{P_0\left[1+\gamma^{(E-D)}+\ldots+\gamma^{(m-1)(E-D)}\right]-P_0\left[1+\gamma^{(E-D_d)}+\ldots+\gamma^{(i-1)(E-D_d)}\right]}{P_0\left[1+\gamma^{(E-D)}+\ldots+\gamma^{(m-1)(E-D)}\right]},$$
$$= \frac{\left(\left(1-(\gamma)^{m(E-D)}\right)/\left(1-\gamma^{(E-D)}\right)\right)-\left(\left(1-(\gamma)^{i(E-D_d)}\right)/\left(1-\gamma^{(E-D_d)}\right)\right)}{\left(\left(1-(\gamma)^{m(E-D)}\right)/\left(1-\gamma^{(E-D)}\right)\right)} = 1-\left[\frac{1-\gamma^{(E-D)}}{1-\gamma^{(E-D_d)}}\right]\left[\frac{1-(\gamma)^{i(E-D_d)}}{\phi}\right]. \quad (17)$$

Considering $\gamma^i = r_i/r_0$, equation (17) can be simplified as

$$\theta_i = \phi - \left[\frac{1-\gamma^{(E-D)}}{1-\gamma^{(E-D_d)}}\right]\left[1-\left(\frac{r_i}{r_0}\right)^{(E-D_d)}\right] \quad (r_m \le r_i \le r_0), \quad (18)$$

when r_i is set to r_0, which means pores with a radius larger than r_0 are drained (i.e., no pores are drained), the water content is equal to the porosity which coincides with the fully saturated condition. The residual volumetric water constant (θ_m) can be calculated when r_i is set to r_m:

$$\theta_m = \phi - \left[\frac{1-\gamma^{(E-D)}}{1-\gamma^{(E-D_d)}}\right]\left[1-(1-\phi)^{(E-D_d)/(E-D)}\right], \quad (19)$$

when r_i is set to r_m, pores with a radius larger than r_m are drained (i.e., the entire interparticle pores) except from those isolated pores. If $D = D_d$ (i.e., no isolated pores), $\theta_m = 0$, which coincides with the dried condition (i.e., only intraparticle water exists).

Therefore, the effective degree of saturation (S_e) can be written by combining equations (18) and (19):

$$S_e = \frac{\theta_i - \theta_m}{\phi - \theta_m} = \frac{(r_i/r_0)^{(E-D_d)} - (1-\phi)^{(E-D_d)/(E-D)}}{1-(1-\phi)^{(E-D_d)/(E-D)}}. \quad (20)$$

Applying the Young–Laplace equation (i.e., $s = \sigma^{lg}/r$, σ^{lg} is the liquid-gas interfacial tension) to equation (18) yields

$$S_e = \begin{cases} 1, & s \le s_{ae}, \\ \dfrac{(s/s_{ae})^{(D_d-E)} - (1-\phi)^a}{1-(1-\phi)^a}, & s_{ae}(1-\phi)^{1/(D-E)} > s > s_{ae}, \\ 0, & s \ge s_{ae}(1-\phi)^{1/(D-E)}, \end{cases} \quad (21)$$

where a is equal to $(D_d - E)/(D - E)$, s is the matric suction or capillary potential, and s_{ae} is the air-entry value, which is inversely proportion to r_0. If s_{ae} is associated with r_0 and s^*_{ae} with r^*_0, then according to (12), we have

$$s_{ae} = s^*_{ae}\left(\frac{1-\phi^*}{1-\phi}\right)^{1/(D-E)}. \quad (22)$$

Substituting equation (22) into equation (21) produces

$$S_e = \begin{cases} 1, & s \le s^*_{ae}\left(\frac{1-\phi^*}{1-\phi}\right)^{1/(D-E)}, \\ \dfrac{(s/s^*_{ae})^{(D_d-E)} - (1-\phi^*)^a}{\left((1-\phi^*)/(1-\phi)\right)^a - (1-\phi^*)^a}, & s^*_{ae}(1-\phi^*)^{1/(D-E)} > s > s^*_{ae}\left(\frac{1-\phi^*}{1-\phi}\right)^{1/(D-E)}, \\ 0, & s \ge s^*_{ae}(1-\phi^*)^{1/(D-E)}, \end{cases} \quad (23)$$

if $D_d = D$ and $\phi^* = \phi$, equation (23) degenerates back to the renown fractal SWRC model proposed by Rieu and Sposito [22]:

$$S_e = \begin{cases} 1, & s \le s_{ae}, \\ \dfrac{1}{\phi}\left(\dfrac{s}{s_{ae}}\right)^{(D-E)} - \dfrac{1}{\phi} + 1, & s_{ae}(1-\phi)^{1/(D-E)} > s > s_{ae}, \\ 0, & s \ge s_{ae}(1-\phi)^{1/(D-E)}. \end{cases} \quad (24)$$

2.3. Porosity-Dependent HCF. The hydraulic conductivity function (HCF) plays a pivotal role in the flow and transport processes under both saturated and unsaturated conditions. The HCF for unsaturated soils is usually represented by the relative hydraulic conductivity K_r, which is defined as the ratio between the unsaturated hydraulic conductivity K and the corresponding saturated hydraulic conductivity K_s. A number of methods have been proposed to quantify the relative hydraulic conductivity K_r for unsaturated soils [7, 12, 19, 59–61], and most of them express K_r as a function of the effective degree of saturation (S_e), volumetric water content (θ),

and matric suction (s). Among the proposed HCFs for unsaturated soils, the most cited HCF is that proposed by Mualem [7]:

$$K_r = \sqrt{S_e}\left(\frac{\int_0^{S_e}(1/s)dS_e}{\int_0^1(1/s)dS_e}\right)^2. \quad (25)$$

When using the model of Mualem [7], the resulting closed-form analytical expression for HCF depends on the model that is used to describe the SWRC. If the SWRC involved is porosity dependent, the HCF is able to reflect the porosity dependency of the unsaturated hydraulic conductivity. Substituting equation (23) into equation (25) generates the fractal model for a soil's K_r and s relationship considering the influence of various soil porosities:

$$K_r = \begin{cases} 1, & s \le s_{ae}^*\left(\dfrac{1-\phi^*}{1-\phi}\right)^{1/(D-E)}, \\ \left[\dfrac{(s/s_{ae}^*)^{(D_d-E)} - (1-\phi^*)^a}{((1-\phi^*)/(1-\phi))^a - (1-\phi^*)^a}\right]^{0.5}\left[\dfrac{(s/s_{ae}^*)^{(D_d-E-1)} - (1-\phi^*)^b}{((1-\phi^*)/(1-\phi))^b - (1-\phi^*)^b}\right]^2, & s_{ae}^*(1-\phi^*)^{1/(D-E)} > s > s_{ae}^*\left(\dfrac{1-\phi^*}{1-\phi}\right)^{1/(D-E)}, \\ 0, & s \ge s_{ae}^*(1-\phi^*)^{1/(D-E)}, \end{cases} \quad (26)$$

where b is equal to $(D_d - E - 1)/(D - E)$.

3. Experimental Validations

3.1. SWRCs with Different Initial Porosities. A series of drying tests on a compacted till were reported by Vanapalli et al. [62]. The soil specimens were compacted to different initial void ratios at the optimum water content. Figures 3(a)–3(d) show the drying test results for these specimens, by different symbols for different initial void ratios (e) or initial porosities (ϕ). The test data with an initial void ratio of 0.517 ($\phi^* = 0.341$) were adopted to calibrate the parameters using the method of least squares. The values of D and D_d can be determined by maximising the value of R^2 when the air-entry value s_{ae}^* is set to 8 kPa according to the data points:

$$R^2 = 1 - \frac{\sum_1^j\left(S_e^{Cal} - S_e^{Exp}\right)^2}{\sum_1^j\left(S_e^{Cal} - \overline{S}_e^{Cal}\right)^2}, \quad (27)$$

where j is the number of experimental data points (in this case, $j = 11$), S_e^{Exp} is the measured (experimental) effective degree of saturation for a data point, and S_e^{Cal} is the calculated effective degree of saturation for a data point for the same data point by equation (23). $\overline{S}_e^{Cal}$ is the mean of the calculated effective degree of saturation for all data points. For all the cases in this study, the Euclidean dimension E is set to 2. Thus, we have the range of D_d and D as $1 < D_d \le D < 2$. The initial values of D_d and D are set to 1, and the increment for D_d and D is set to 10^{-3} (i.e., $\Delta D_d = \Delta D = 10^{-3}$). For each set of D_d and D, a value R^2 is calculated and recorded. Finally, the maximum value of R^2 can be achieved, which is equal to 0.9837, when $D_d = 1.915$ and $D = 1.972$. The other 3 data sets (corresponding to $e = 0.514$, $e = 0.474$, and $e = 0.444$) were used to validate the proposed equation. The predicted SWRCs were calculated using equation (23) and are shown as solid curves in Figure 3. The value of R^2 for rest three data sets is computed to illustrate the validity of the model predictions. The predicted SWRCs in Figures 3(b)–3(d) match the experimental data well with R^2 varying from 0.9364 to 0.9726, indicating that the proposed fractal approach captures the effects of the initial void ratio on the SWRCs well.

A series of laboratory experiments were conducted by Huang et al. [63] to investigate the water retention behaviour of a deformable unsaturated soil. The soil tested was silty sand from the Saskatchewan Department of Highway borrow pit. This silty sand consisted of 52.5% sand, 37.5% silt, and 10% clay. The specific gravity, liquid limit, and plastic limit were 2.68, 22.2%, and 16.6%, respectively. The air-dried silty sand was mixed with distilled water to prepare slurried specimens for the experimental program. Six initially slurried specimens (grouped as PPCT2) were one-dimensionally preconsolidated under different pressures to obtain different initial void ratios for the water retention tests. The test results are replotted in the S_e-s plane together with the predictions of equation (23) in Figures 4(a)–4(f). The water retention test data for an initial void ratio of 0.525 ($\phi^* = 0.344$) were used to calibrate the parameters. The values of D (=1.883) and D_d (=1.883) were determined by maximising the value of R^2 (=0.9966) when the air-entry value s_{ae}^* set to 24 kPa according to the data points. As shown in Figures 4(b)–4(f), the predicted SWRCs agree very well with the experimental SWRCs ($R^2 = 0.9821$~0.9968).

Very recently, Salager et al. [64] conducted a series of tests on a clayey sand to investigate the water retention behaviour of a granular soil. The tested soil consisted of 72% sand, 18% silt, and 10% clay. The water retention behaviour of the clayey sand compacted at five different void ratios (e) is replotted in the S_e-s plane in Figures 5(a)–5(e). The variation in the initial void ratios ranges from 0.44 to 1.01.

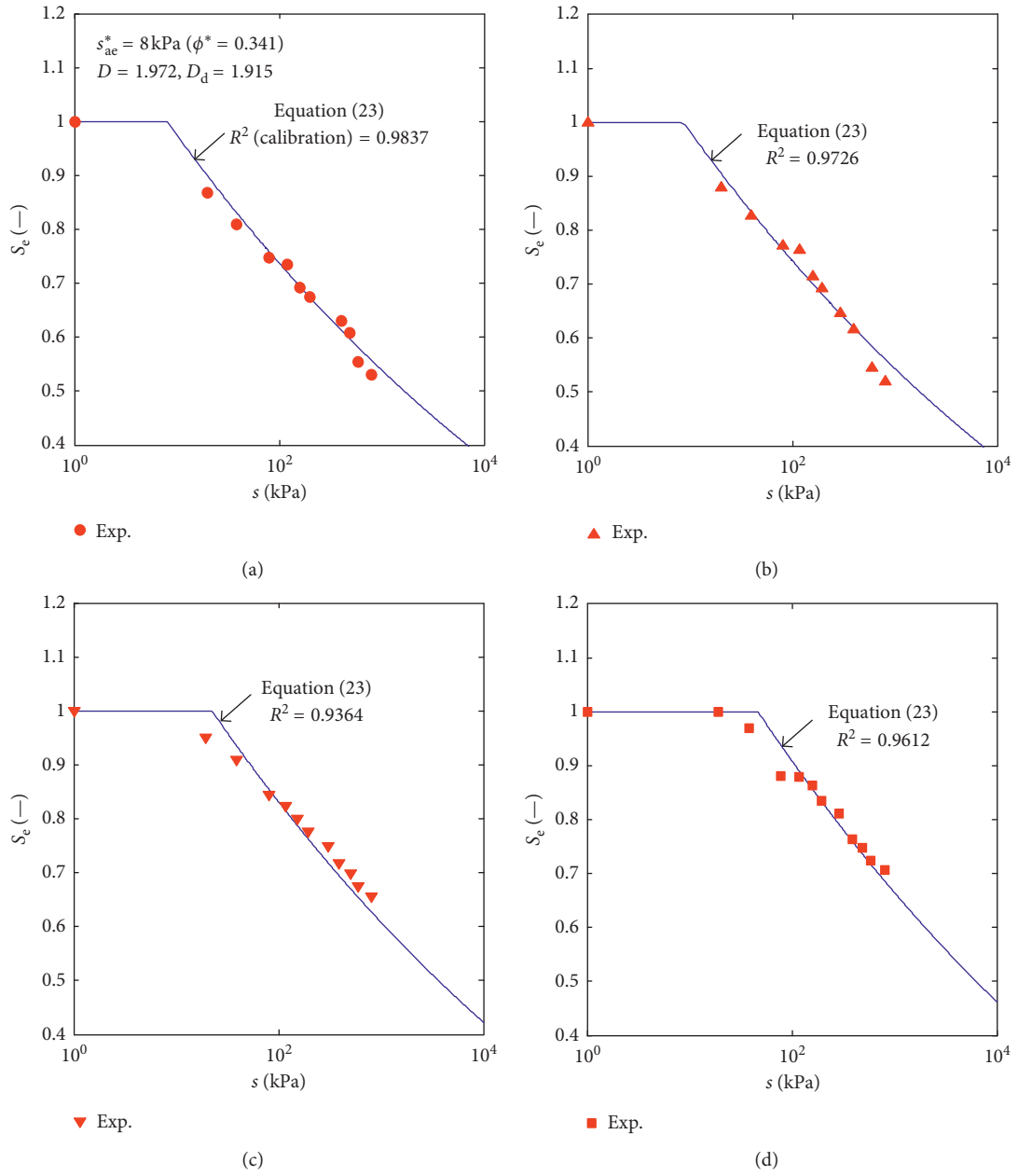

FIGURE 3: Measured and predicted SWRCs for specimens compacted at optimum water content (data after Vanapalli et al. [62]): (a) $e = 0.517$; (b) $e = 0.514$; (c) $e = 0.474$; (d) $e = 0.444$.

The water retention data for the loosest specimen ($e^* = 1.01$, i.e., $\phi^* = 0.502$) were adopted to calibrate the parameters. The values of D (=1.951) and D_d (=1.935) were determined by maximising the value of R^2 (=0.9834) when the air-entry value s^*_{ae} is set to 0.2 kPa according to the data points. The SWRCs predicted by equation (23) are shown in Figures 5(b)–5(e). Again, the comparison between the experimental data and predictions is of acceptable accuracy with the value of R^2 between 0.8865 and 0.9794.

3.2. HCFs with Different Initial Porosities. Laliberte et al. [26] measured the SWRCs (S_e versus s) and HCFs (K_r versus s) of a silt loam, which is referred to as the Touchet silt loam, with different initial porosities. A Touchet silt loam is coarse silt, consisting of 32% sand, 53% silt, and 15% clay, with a particle density of 2.599 g/cm^3. The initial porosities for the water retention tests are 0.493 ($e^* = 0.972$), 0.463 ($e = 0.862$), and 0.430 ($e = 0.754$). The initial porosities for the hydraulic conductivity tests are 0.503 ($e = 1.012$), 0.478 ($e = 0.916$), 0.449 ($e = 0.815$), 0.423 ($e = 0.733$), and 0.395 ($e = 0.653$). The data set for the loosest specimen ($\phi^* = 0.493$) of the water retention test is used for calibration. The parameters for SWRC are set to $s^*_{ae} = 4.5$ kPa, $D = 1.7$, and $D_d = 1.05$, which result in a value of $R^2 = 0.9909$ for all data sets with three different initial porosities (Figure 6(a)). As shown in

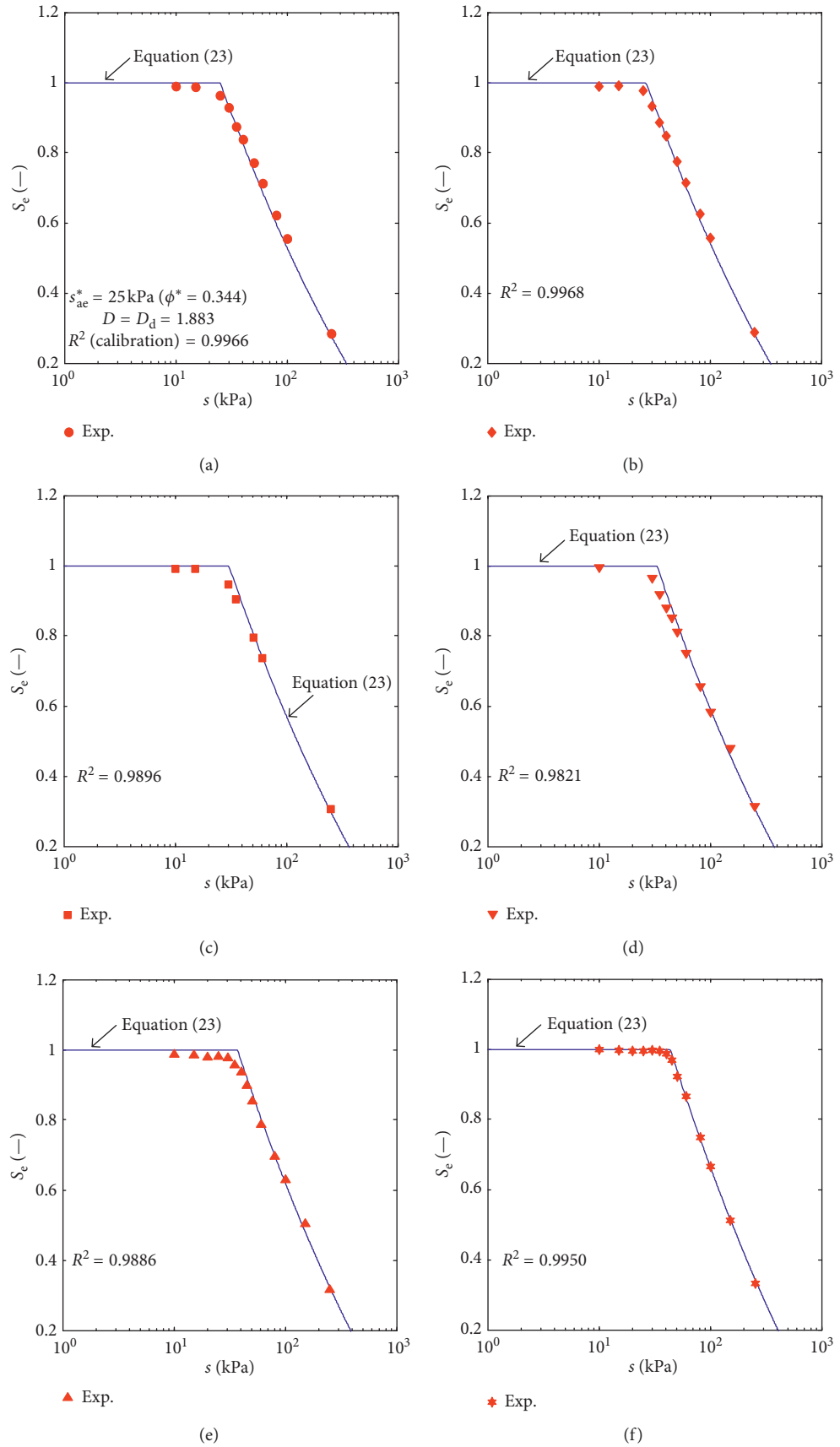

Figure 4: Measured and predicted SWRCs for silty sand with different initial void ratios (data after Huang et al. [63]): (a) $e = 0.525$; (b) $e = 0.513$; (c) $e = 0.490$; (d) $e = 0.474$; (e) $e = 0.454$; (f) $e = 0.426$.

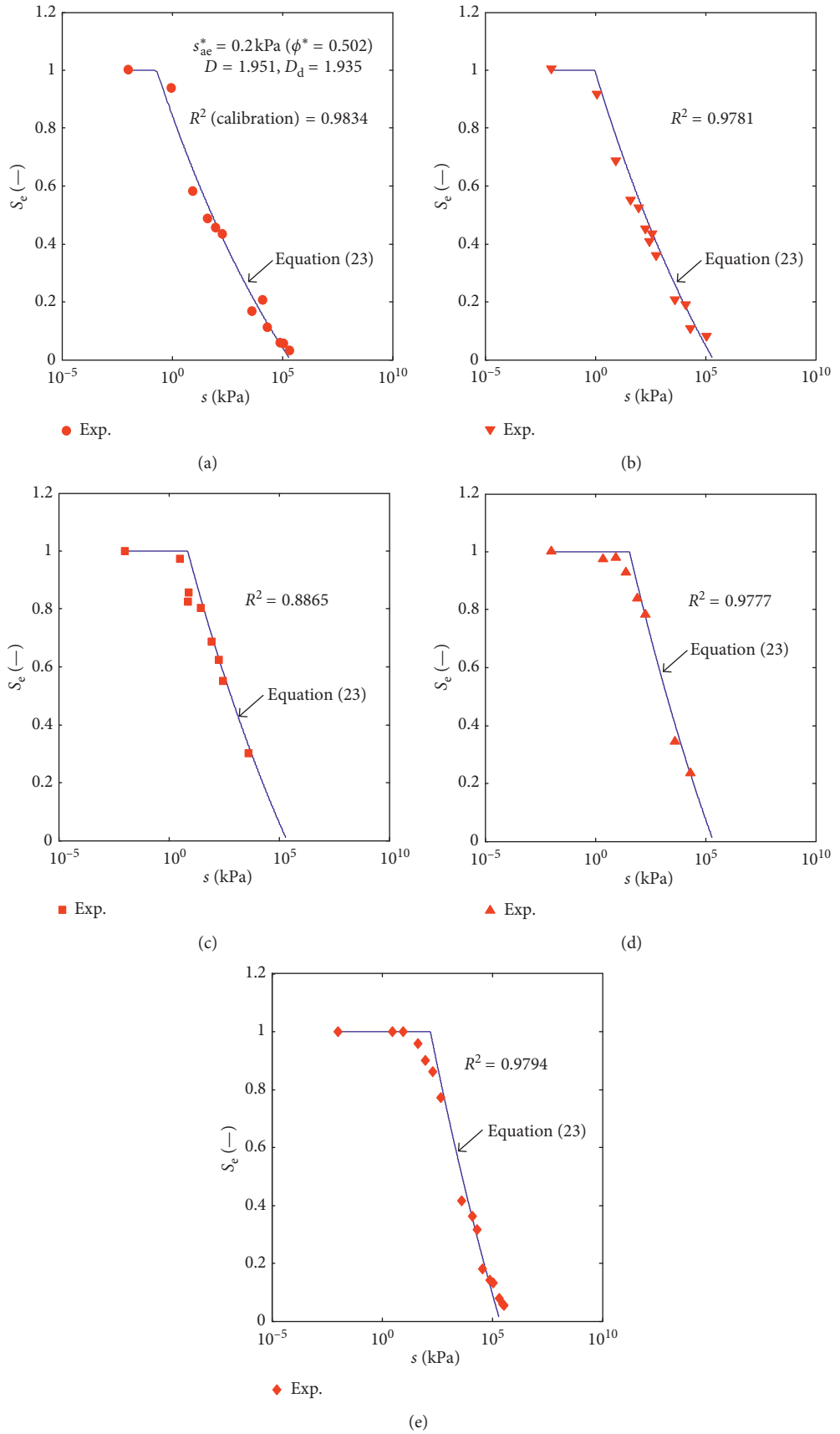

Figure 5: Measured and predicted family of SWRCs for a clayey sand with different initial void ratios (data after Salager et al. [64]): (a) $e = 1.01$; (b) $e = 0.86$; (c) $e = 0.68$; (d) $e = 0.55$; (e) $e = 0.44$.

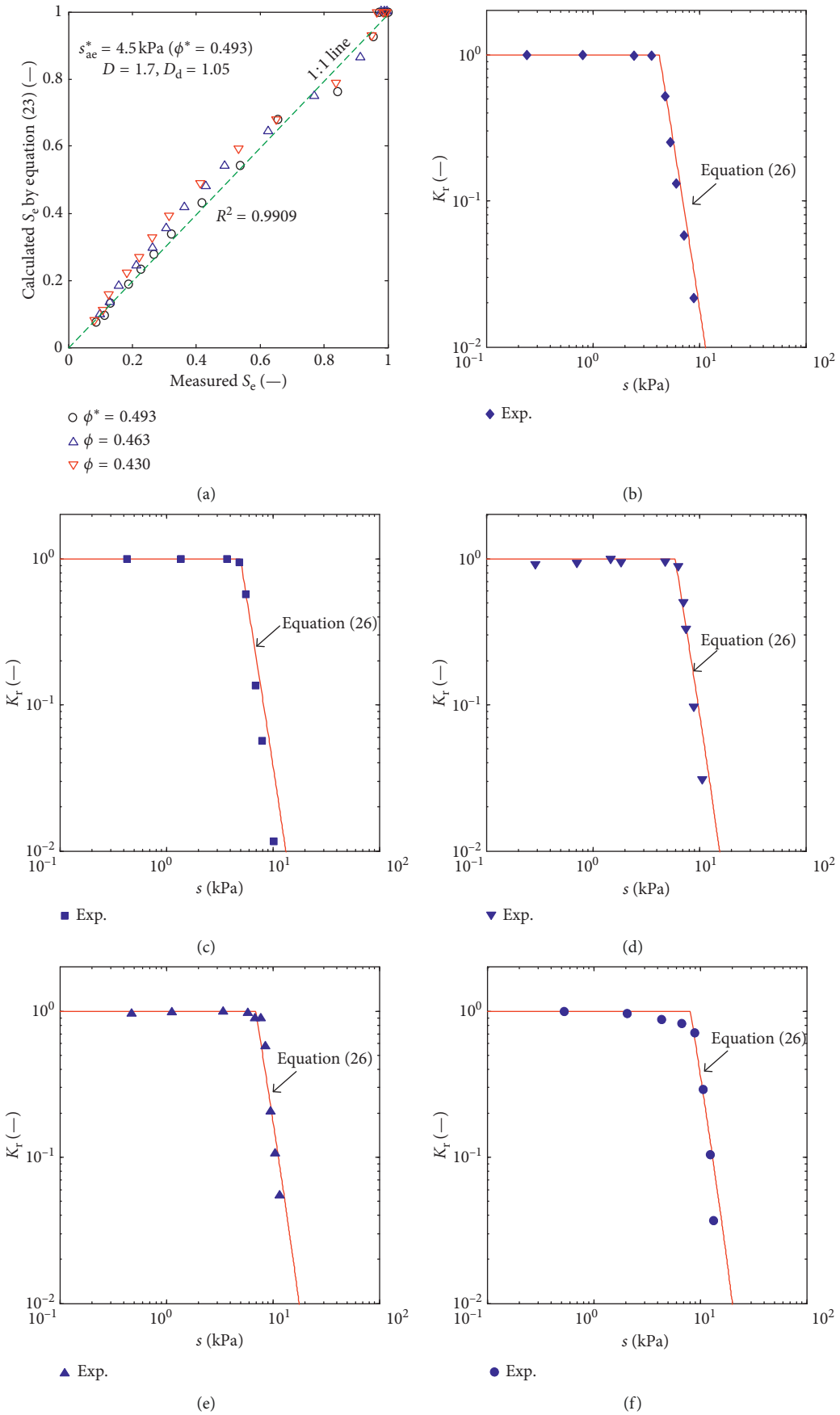

FIGURE 6: Comparison between measured and predicted SWRCs and HCFs for the Touchet silt loam: (a) SWRCs, (b) HCF ($\phi = 0.503$), (c) HCF ($\phi = 0.478$), (d) HCF ($\phi = 0.449$), (e) HCF ($\phi = 0.423$), and (f) HCF ($\phi = 0.395$).

Figures 6(b)–6(f), the measured relative hydraulic conductivities for five different initial porosities (0.503~0.395) are replotted in the K_r-s plane (double logarithmic scales), which are the predictions obtained using equation (26). The predicted K_r-s curves agree with the experimental data reasonably well, which confirms that the proposed porosity-dependent fractal HCF model (i.e., equation (26)) captures well the effects of the initial porosity on the soil's unsaturated permeability.

4. Conclusions

A simple physical model based on fractal geometry was proposed to quantify the effects of initial porosity on the soil-water retention curve (SWRC) and the hydraulic conductivity function (HCF) for unsaturated porous media. The proposed fractal model involves three parameters: (1) the air-entry value that is related to the size of the maximum pores, (2) the fractal dimension of pore volume (D), and (3) the fractal dimension of drainable pore volume (D_d). The range of D and D_d is limited to between $E - 1$ and E (i.e., Euclidean dimension). The difference between D and D_d ($D \geq D_d$) implies that incomplete pore connectivity may exist in the porous medium. The values of D and D_d can be calibrated conveniently using one data set of the water retention tests at initial porosity. A regression analysis using the method of least squares indicates that the proposed model is valid to reproduce the porosity-dependent SWRCs and HCFs for a variety of unsaturated soils.

Data Availability

The data used to support the findings of this study are included within the article.

Conflicts of Interest

The authors declare that they have no conflicts of interest.

Acknowledgments

This research was financially supported by the National Natural Science Foundation of China (51679004).

References

[1] S.-L. Shen, Z.-F. Wang, J. Yang, and C.-E. Ho, "Generalized approach for prediction of jet grout column diameter," *Journal of Geotechnical and Geoenvironmental Engineering*, vol. 139, no. 12, pp. 2060–2069, 2013.

[2] S.-L. Shen, J.-P. Wang, H.-N. Wu, Y.-S. Xu, G.-L. Ye, and Z.-Y. Yin, "Evaluation of hydraulic conductivity for both marine and deltaic deposits based on piezocone testing," *Ocean Engineering*, vol. 110, pp. 174–182, 2015.

[3] S.-L. Shen, Y.-X. Wu, Y.-S. Xu, T. Hino, and H.-N. Wu, "Evaluation of hydraulic parameters from pumping tests in multi-aquifers with vertical leakage in Tianjin," *Computers and Geotechnics*, vol. 68, pp. 196–207, 2015.

[4] S. L. Shen, Z. F. Wang, and W. C. Cheng, "Estimation of lateral displacement induced by jet grouting in clayey soils," *Géotechnique*, vol. 67, no. 7, pp. 621–630, 2017.

[5] S.-L. Shen, Y.-X. Wu, and A. Misra, "Calculation of head difference at two sides of a cut-off barrier during excavation dewatering," *Computers and Geotechnics*, vol. 91, pp. 192–202, 2017.

[6] Y.-S. Xu, H.-N. Wu, J. S. Shen, and N. Zhang, "Risk and impacts on the environment of free-phase biogas in quaternary deposits along the coastal region of Shanghai," *Ocean Engineering*, vol. 137, pp. 129–137, 2017.

[7] Y. Mualem, "A new model for predicting the hydraulic conductivity of unsaturated porous media," *Water Resources Research*, vol. 12, no. 3, pp. 513–522, 2010.

[8] R. Brooks and A. Corey, *Hydraulic Properties of Porous Media*, Colorado State University, Fort Collins, CO, USA, 1964.

[9] D. G. Fredlund and A. Xing, "Equations for the soil-water characteristic curve," *Canadian Geotechnical Journal*, vol. 31, no. 4, pp. 521–532, 1994.

[10] W. Gardner, "Mathematics of isothermal water conduction in unsaturated soils, highway research board special report 40," in *Proceedings of International Symposium on Physico-Chemical Phenomenon in Soils*, pp. 78–87, Washington, DC, USA, 1956.

[11] M. T. van Genuchten, "A closed-form equation for predicting the hydraulic conductivity of unsaturated soils 1," *Soil Science Society of America Journal*, vol. 44, no. 5, pp. 892–898, 1980.

[12] S. Assouline, "A model for soil relative hydraulic conductivity based on the water retention characteristic curve," *Water Resources Research*, vol. 37, no. 2, pp. 265–271, 2001.

[13] N. T. Burdine, "Relative permeability calculations from pore size distribution data," *Journal of Petroleum Technology*, vol. 5, no. 3, pp. 71–78, 2013.

[14] D. G. Fredlund, A. Xing, and S. Huang, "Equations for the soil-water characteristic curve," *Canadian Geotechnical Journal*, vol. 31, no. 4, pp. 521–532, 1994.

[15] S. W. Tyler and S. W. Wheatcraft, "Fractal processes in soil water retention," *Water Resources Research*, vol. 26, no. 5, pp. 1047–1054, 2010.

[16] N. R. A. Bird, E. Perrier, and M. Rieu, "The water retention function for a model of soil structure with pore and solid fractal distributions," *European Journal of Soil Science*, vol. 51, no. 1, pp. 55–63, 2008.

[17] A. Cihan, J. S. Tyner, and E. Perfect, "Predicting relative permeability from water retention: a direct approach based on fractal geometry," *Water Resources Research*, vol. 45, no. 4, p. W04404, 2009.

[18] C. Fuentes, M. Vauclin, J.-Y. Parlange, and R. Haverkamp, "A note on the soil-water conductivity of a fractal soil," *Transport in Porous Media*, vol. 23, no. 1, pp. 31–36, 1996.

[19] Y. A. Pachepsky, R. A. Shcherbakov, and L. P. Korsunskaya, "Scaling of soil water retention using a fractal model," *Soil Science*, vol. 159, no. 2, pp. 99–104, 1995.

[20] E. Perfect, N. B. McLaughlin, B. D. Kay, and G. C. Topp, "An improved fractal equation for the soil water retention curve," *Water Resources Research*, vol. 32, no. 2, pp. 281–287, 1996.

[21] E. Perrier, M. Rieu, G. Sposito, and G. de Marsily, "Models of the water retention curve for soils with a fractal pore size distribution," *Water Resources Research*, vol. 32, no. 10, pp. 3025–3031, 1996.

[22] M. Rieu and G. Sposito, "Fractal fragmentation, soil porosity, and soil water properties: I. Theory," *Soil Science Society of America Journal*, vol. 55, no. 5, pp. 1231–1238, 1991.

[23] Y. Xu, "Calculation of unsaturated hydraulic conductivity using a fractal model for the pore-size distribution," *Computers and Geotechnics*, vol. 31, no. 7, pp. 549–557, 2004.

[24] Y. F. Xu and D. A. Sun, "A fractal model for soil pores and its application to determination of water permeability," *Physica A: Statistical Mechanics and its Applications*, vol. 316, no. 1-4, pp. 56–64, 2002.
[25] D. Croney and J. D. Coleman, "Soil structure in relation to soil suction (pF)," *Journal of Soil Science*, vol. 5, no. 1, pp. 75–84, 2006.
[26] G. E. Laliberte, A. Corey, and R. Brooks, *Properties of Unsaturated Porous Media*, Colorado State University, Fort Collins, CO, USA, 1966.
[27] S. Assouline, "Modeling the relationship between soil bulk density and the water retention curve," *Vadose Zone Journal*, vol. 5, no. 2, pp. 554–562, 2006.
[28] D. Gallipoli, S. J. Wheeler, and M. Karstunen, "Modelling the variation of degree of saturation in a deformable unsaturated soil," *Géotechnique*, vol. 53, no. 1, pp. 105–112, 2003.
[29] T. Luo, Y.-P. Yao, A.-N. Zhou, and X.-G. Tian, "A three-dimensional criterion for asymptotic states," *Computers and Geotechnics*, vol. 41, pp. 90–94, 2012.
[30] D. Masin, "Predicting the dependency of a degree of saturation on void ratio and suction using effective stress principle for unsaturated soils," *International Journal for Numerical and Analytical Methods in Geomechanics*, vol. 34, pp. 73–90, 2010.
[31] M. Nuth and L. Laloui, "Advances in modelling hysteretic water retention curve in deformable soils," *Computers and Geotechnics*, vol. 35, no. 6, pp. 835–844, 2008.
[32] Y. Yao, W. Hou, and A. Zhou, "Constitutive model for overconsolidated clays," *Science in China Series E: Technological Sciences*, vol. 51, no. 2, pp. 179–191, 2008.
[33] A. Zhou and D. Sheng, "An advanced hydro-mechanical constitutive model for unsaturated soils with different initial densities," *Computers and Geotechnics*, vol. 63, pp. 46–66, 2015.
[34] A.-N. Zhou, D. Sheng, S. W. Sloan, and A. Gens, "Interpretation of unsaturated soil behaviour in the stress-saturation space, I: volume change and water retention behaviour," *Computers and Geotechnics*, vol. 43, pp. 178–187, 2012.
[35] A. Zhou, D. Sheng, S. W. Sloan, and A. Gens, "Modelling volume change behaviour for unsaturated soils in the stress-saturation space," *Unsaturated Soils: Research and Applications*, vol. 43, pp. 111–118, 2012.
[36] A.-N. Zhou, D. Sheng, and J. Li, "Modelling water retention and volume change behaviours of unsaturated soils in non-isothermal conditions," *Computers and Geotechnics*, vol. 55, pp. 1–13, 2014.
[37] A. Zhou, S. Wu, J. Li, and D. Sheng, "Including degree of capillary saturation into constitutive modelling of unsaturated soils," *Computers and Geotechnics*, vol. 95, pp. 82–98, 2018.
[38] A.-N. Zhou, "A contact angle-dependent hysteresis model for soil-water retention behaviour," *Computers and Geotechnics*, vol. 49, pp. 36–42, 2013.
[39] S. Assouline, "Modeling the relationship between soil bulk density and the hydraulic conductivity function," *Vadose Zone Journal*, vol. 5, no. 2, pp. 697–705, 2006.
[40] D. A. Sun, D. Sheng, and S. W. Sloan, "Elastoplastic modelling of hydraulic and stress-strain behaviour of unsaturated soils," *Mechanics of Materials*, vol. 39, no. 3, pp. 212–221, 2007.
[41] D. A. Sun, D. Sheng, and Y. Xu, "Collapse behaviour of unsaturated compacted soil with different initial densities," *Canadian Geotechnical Journal*, vol. 44, no. 6, pp. 673–686, 2007.
[42] A. Tarantino, "A water retention model for deformable soils," *Géotechnique*, vol. 59, no. 9, pp. 751–762, 2009.
[43] D. Sheng and A.-N. Zhou, "Coupling hydraulic with mechanical models for unsaturated soils," *Canadian Geotechnical Journal*, vol. 48, no. 5, pp. 826–840, 2011.
[44] A.-N. Zhou, D. Sheng, and J. P. Carter, "Modelling the effect of initial density on soil-water characteristic curves," *Géotechnique*, vol. 62, no. 8, pp. 669–680, 2012.
[45] D. A. Sun, D. Sheng, L. Xiang, and S. W. Sloan, "Elastoplastic prediction of hydro-mechanical behaviour of unsaturated soils under undrained conditions," *Computers and Geotechnics*, vol. 35, no. 6, pp. 845–852, 2008.
[46] A. Tarantino, "Unsaturated soils: compacted versus reconstituted states," in *Unsaturated Soils*, E. E. Alonso and A. Gens, Eds., pp. 113–136, CRC Press, Barcelona, Spain, 2011.
[47] A. Zhou, R. Huang, and D. Sheng, "Capillary water retention curve and shear strength of unsaturated soils," *Canadian Geotechnical Journal*, vol. 53, no. 6, pp. 974–987, 2016.
[48] E. Romero and P. H. Simms, "Microstructure investigation in unsaturated soils: a review with special attention to contribution of mercury intrusion porosimetry and environmental scanning electron microscopy," *Geotechnical and Geological Engineering*, vol. 26, no. 6, pp. 705–727, 2008.
[49] B. B. Mandelbrot, *The Fractal Geometry of Nature*, WH Freeman and Co., New York, NY, USA, 1983.
[50] D. Giménez, E. Perfect, W. J. Rawls, and Y. Pachepsky, "Fractal models for predicting soil hydraulic properties: a review," *Engineering Geology*, vol. 48, pp. 161–183, 1997.
[51] Y. Xu, "The fractal evolution of particle fragmentation under different fracture energy," *Powder Technology*, vol. 323, pp. 337–345, 2018.
[52] Y. Xu, "Shear strength of granular materials based on fractal fragmentation of particles," *Powder Technology*, vol. 333, pp. 1–8, 2018.
[53] A. J. Katz and A. H. Thompson, "Fractal sandstone pores: implications for conductivity and pore formation," *Physical Review Letters*, vol. 54, no. 12, pp. 1325–1328, 1985.
[54] A. G. Hunt, "Comments on "fractal fragmentation, soil porosity, and soil water properties: I. Theory"," *Soil Science Society of America Journal*, vol. 71, no. 4, pp. 1418-1419, 2007.
[55] Y. Xu and X. Xia, "Fractal model for virgin compression of pure clays," *Mechanics Research Communications*, vol. 33, no. 2, pp. 206–216, 2006.
[56] A. Cihan, E. Perfect, and J. S. Tyner, "Water retention models for scale-variant and scale-invariant drainage of mass prefractal porous media," *Vadose Zone Journal*, vol. 6, no. 4, pp. 786–792, 2007.
[57] E. Perfect, "Modeling the primary drainage curve of prefractal porous media," *Vadose Zone Journal*, vol. 4, no. 4, pp. 959–966, 2005.
[58] J. W. Crawford, N. Matsui, and I. M. Young, "The relation between the moisture-release curve and the structure of soil," *European Journal of Soil Science*, vol. 46, no. 3, pp. 369–375, 1995.
[59] G. Cai, A. Zhou, and D. Sheng, "Permeability function for unsaturated soils with different initial densities," *Canadian Geotechnical Journal*, vol. 51, no. 12, pp. 1456–1467, 2014.
[60] G. S. Campbell, "A simple method for determining unsaturated conductivity from moisture retention data," *Soil Science*, vol. 117, no. 6, pp. 311–314, 1974.
[61] J. Stolte, J. M. Halbertsma, G. J. Veerman et al., "Comparison of six methods to determine unsaturated soil hydraulic conductivity," *Soil Science Society of America Journal*, vol. 58, no. 6, pp. 1596–1603, 1994.
[62] S. K. Vanapalli, D. G. Fredlund, and D. E. Pufahl, "The influence of soil structure and stress history on the soil-water characteristics of a compacted till," *Géotechnique*, vol. 49, no. 2, pp. 143–159, 1999.
[63] S. Huang, S. L. Barbour, and D. G. Fredlund, "Development and verification of a coefficient of permeability function for a

deformable unsaturated soil," *Canadian Geotechnical Journal*, vol. 35, no. 3, pp. 411–425, 1998.

[64] S. Salager, M. S. El Youssoufi, and C. Saix, "Definition and experimental determination of a soil-water retention surface," *Canadian Geotechnical Journal*, vol. 47, no. 6, pp. 609–622, 2010.